

SAND REPORT

SAND200-0397

Unlimited Release

Printed February 2003

Molecular Dynamics Simulation of Polymer Dissolution

Aidan P. Thompson

Prepared by
Sandia National Laboratories
Albuquerque, New Mexico 87185 and Livermore, California 94550

Sandia is a multiprogram laboratory operated by Sandia Corporation,
a Lockheed Martin Company, for the United States Department of Energy's
National Nuclear Security Administration under Contract DE-AC04-94-AL85000.

Approved for public release; further dissemination unlimited.



Issued by Sandia National Laboratories, operated for the United States Department of Energy by Sandia Corporation.

NOTICE: This report was prepared as an account of work sponsored by an agency of the United States Government. Neither the United States Government, nor any agency thereof, nor any of their employees, nor any of their contractors, subcontractors, or their employees, make any warranty, express or implied, or assume any legal liability or responsibility for the accuracy, completeness, or usefulness of any information, apparatus, product, or process disclosed, or represent that its use would not infringe privately owned rights. Reference herein to any specific commercial product, process, or service by trade name, trademark, manufacturer, or otherwise, does not necessarily constitute or imply its endorsement, recommendation, or favoring by the United States Government, any agency thereof, or any of their contractors or subcontractors. The views and opinions expressed herein do not necessarily state or reflect those of the United States Government, any agency thereof, or any of their contractors.

Printed in the United States of America. This report has been reproduced directly from the best available copy.

Available to DOE and DOE contractors from

U.S. Department of Energy
Office of Scientific and Technical Information
P.O. Box 62
Oak Ridge, TN 37831

Telephone: (865)576-8401
Facsimile: (865)576-5728
E-Mail: reports@adonis.osti.gov
Online ordering: <http://www.doe.gov/bridge>

Available to the public from

U.S. Department of Commerce
National Technical Information Service
5285 Port Royal Rd
Springfield, VA 22161

Telephone: (800)553-6847
Facsimile: (703)605-6900
E-Mail: orders@ntis.fedworld.gov
Online order: <http://www.ntis.gov/help/ordermethods.asp?loc=7-4-0#online>



SAND 2003-0397
Unlimited Release
Printed February 2003

Molecular Dynamics Simulation of Polymer Dissolution

Aidan P. Thompson

Computational Materials & Molecular Biology
Sandia National Laboratories
P.O. Box 5800, MS 0316
Albuquerque, NM 87185-0316

Abstract

In the LIGA process for manufacturing microcomponents, a polymer film is exposed to an x-ray beam passed through a gold pattern. This is followed by the development stage, in which a selective solvent is used to remove the exposed polymer, reproducing the gold pattern in the polymer film. Development is essentially polymer dissolution, a physical process which is not well understood. We have used coarse-grained molecular dynamics simulation to study the early stage of polymer dissolution. In each simulation a film of non-glassy polymer was brought into contact with a layer of solvent. The mutual penetration of the two phases was tracked as a function of time. Several film thicknesses and two different chain lengths were simulated. In all cases, the penetration process conformed to ideal Fickian diffusion. We did not see the formation of a gel layer or other non-ideal effects. Variations in the Fickian diffusivities appeared to be caused primarily by differences in the bulk polymer film density.

CONTENTS

Abstract	3
Introduction	5
Simulation Method	5
Results	10
Conclusions	13
References	14

Introduction

The purpose of this document is to report on a preliminary study of polymer dissolution using molecular dynamics simulation. This work was motivated primarily by the need for better models of development kinetics in the LIGA process.¹ LIGA is a German acronym for lithography, electrodeposition and molding. High-resolution, high-aspect ratio features are etched in a PMMA polymer film by first exposing the polymer to a high-energy x-ray beam shone through a gold pattern. The x-rays lower the molecular weight of the PMMA in those regions which are not covered by the gold pattern. In a second step, known as development, a special solvent selectively dissolves the low molecular weight regions of the film, creating a positive image of the gold pattern in the PMMA. The achievable resolution of LIGA parts is to some extent limited by sidewall development *i.e.*, the tendency for the solvent to etch sideways as well as downward.² Improved understanding of PMMA development will lead to better strategies for controlling sidewall development and increasing the achievable resolution.

Development is essentially a dissolution process. A low molecular weight solvent penetrates the polymer film and swells it, allowing the polymer molecules to disentangle, diffuse into the bulk solvent and be transported away by convection. Beyond this brief description, the mechanisms of polymer dissolution are poorly understood, but are believed to be strongly influenced by solvent/polymer interactions at the molecular length scale. In some cases, simple Fickian diffusion is observed *i.e.*, the depth of solvent penetration is linear in the square root of time. However, glassy polymers such as PMMA often exhibit what is known as class II behavior *i.e.*, the depth of solvent penetration is linear in time.³ This is caused by the presence of a sharp front separating the glassy region where the solvent concentration is small and the non-glassy region where the solvent concentration is higher. There is some theoretical and experimental evidence which suggests that a similar front forms in dissolution of non-glassy polymers.^{4,5} Molecular dynamics provides a way to directly simulate polymer dissolution, without making any assumptions about the nature of the transport processes. The only inputs are descriptions of the interaction potentials between particles which represent either solvent molecules or segments of the polymer. Over the years, physically realistic interaction potentials have been developed for polymer/solvent systems. The molecular dynamics code uses the interaction potentials to track the motion of all the particles in the system. The challenge is to devise computer experiments that can reveal physical behavior different from that predicted by a simple Fickian model of solvent penetration.

Simulation Method

To maximize the probability of success, we chose a very simple experiment and a very computationally efficient interaction potential. The system of particles consisted of a rectangular box. One half was filled with N_c linear polymer chains, each consisting of N particles. The other half was filled with N_s solvent particles, so the total number of particles in a simulation was $N_{tot} = N N_c + N_s$. The polymer model was the same as that used by Kremer and Grest⁶ in their study of polymer melt dynamics. This has been shown to provide a good representation of a non-glassy polymer with an entanglement length of about 50 segments. All polymer segments interacted with a soft repulsive interaction which falls smoothly to zero at a separation of $2^{1/6} \sigma$.

$$u_{ij}(r) = \begin{cases} 4\epsilon \left[\left(\frac{\sigma}{r} \right)^{12} - \left(\frac{\sigma}{r} \right)^6 + \frac{1}{4} \right], & r < 2^{1/6} \sigma \\ 0, & r \geq 2^{1/6} \sigma \end{cases} \quad (1)$$

where r is the separation between particles i and j , σ is the particle diameter of the polymer segment, and ϵ is an energy parameter which controls the stiffness of the repulsive interaction. Consecutive polymer segments on the polymer chain are held together by an additional finite-extensible nonlinear elastic (FENE) interaction that becomes increasingly attractive as the bond length increases from zero to a maximum value of R_0 .

$$u_{ij}^b(r) = \begin{cases} -\frac{k_b}{2} R_0^2 \ln \left[1 - \left(\frac{r}{R_0} \right)^2 \right], & r < R_0 \\ \infty, & r \geq R_0 \end{cases} \quad (2)$$

where R_0 is the maximum bond extension and k_b is a stiffness parameter.

For the polymer molecules, we chose the interaction parameters of Kremer and Grest *i.e.*, $\sigma = 1$, $\epsilon = 1$, $R_0 = 1.5$ and $k_b = 30$, where all of these quantities use the same arbitrary units of energy and length. The solvent particles were identical to the polymer segments, which ensured that they formed a good solvent for the polymer.⁷ The masses of the solvent and polymer segments were set to unity; the temperature was maintained at $1.0\epsilon/k_B$, where k_B is Boltzmann's constant. Time was measured in units of $\tau = \sigma(m/\epsilon)^{1/2}$ which is roughly equal to the time required for a particle to travel one particle diameter, based on its average thermal speed.

In all simulations the polymer molecules were initially assembled and equilibrated in a periodic box with dimensions $L_x/2$, L_y , L_z , chosen so that the density of segments was $0.85\sigma^{-3}$, the same as that used by Kremer and Grest. Reflective boundaries were used in the x direction to preserve a flat interface. The length of the periodic box in the x direction was then doubled, with a replica of the polymer used to fill the additional space. The bonds in the replica polymer were removed and the atom types were switched from polymer to solvent. This configuration was used as the starting point for the dissolution simulation. In all stages of the simulation process, a timestep of 0.005τ was used. Temperature was controlled using a Nosé-Hoover thermostat with time constant $40/\tau$.

Table 1 Summary of dissolution simulations.

N	N_c	N_s	N_{tot}	L_x/σ	L_y/σ	L_z/σ	$N_{step} (10^6)$	$D\tau/\sigma^2$	$\rho_{p,eff}\sigma^3$
10	200	2,000	4,000	26.6	13.3	13.3	1.0	-	-
100	20	2,000	4,000	26.6	13.3	13.3	1.0	-	-
10	2,000	20,000	40,000	266.0	13.3	13.3	6.0	0.00594	0.900
100	200	20,000	40,000	266.0	13.3	13.3	5.0	0.00442	0.906
10	20,000	200,000	400,000	2660.0	13.3	13.3	11.0	0.00115	0.919
100	2,000	200,000	400,000	2660.0	13.3	13.3	14.0	0.00091	0.926

We report here on six dissolution simulations that differ only in the choice of N (10, 100) and N_{tot} (4,000, 40,000, 400,000). The system dimensions and run times are tabulated in Table I. All of the simulations were performed using the LAMMPS massively parallel molecular dynamics code.⁸ The largest simulations (400,000 particles) were run on 100 nodes of the Cplant Ross cluster (466 MHz DEC alpha ev6 chips connected by Myrinet).⁹ Throughput was approximately 80 hours to complete 10 million timesteps.

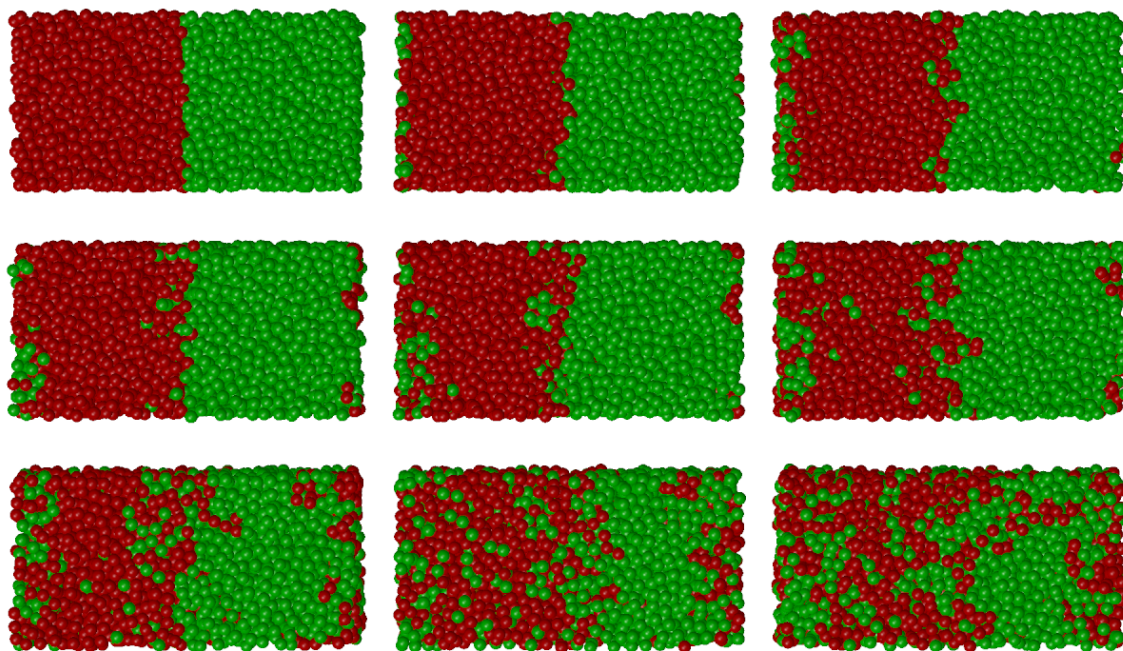


Figure 1 Snapshots of polymer segments (red) solvent particles (green) taken from the smallest polymer dissolution simulation ($N = 100$, $N_{tot} = 4,000$). The snapshots were taken at 0, 1000, 2000, 4000, 8000, 16000, 32000, 64000, and 128000 timesteps.

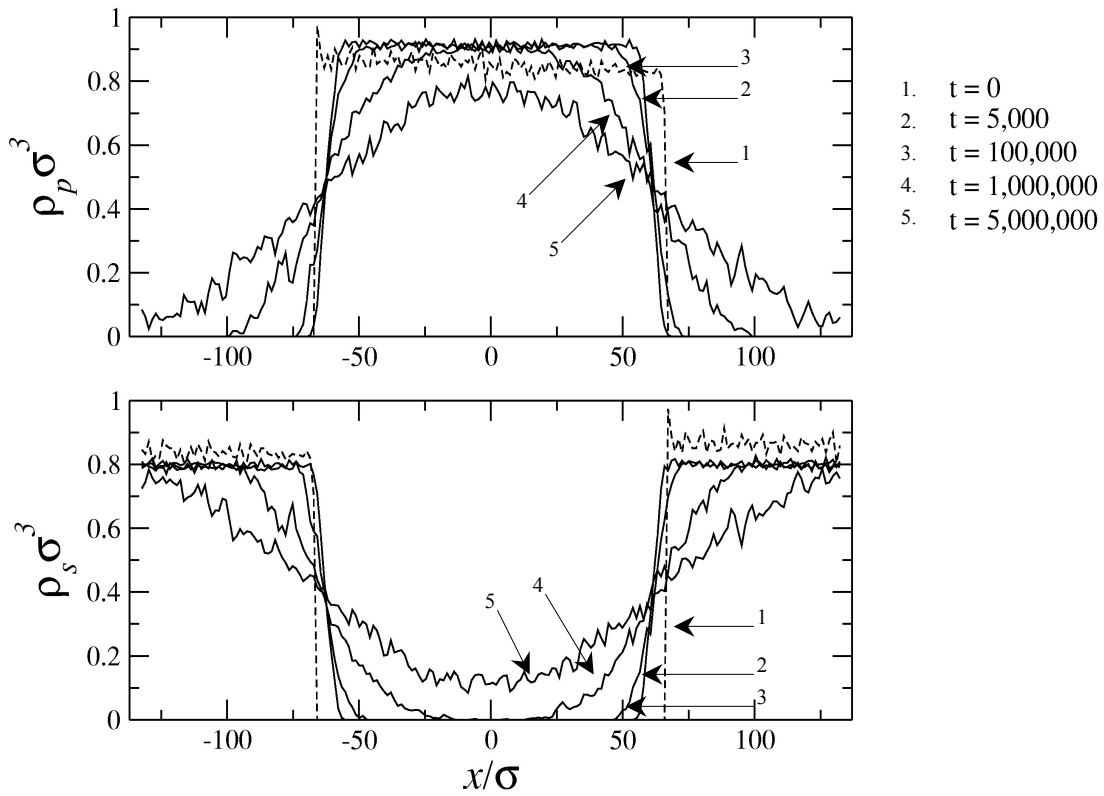


Figure 1 Plot of polymer (top) and solvent (bottom) density profiles for the case ($N = 10$, $N_{tot} = 40,000$). The dashed line is the initial profile. The solid lines correspond to the times listed in the legend. One timestep corresponds to 0.005τ .

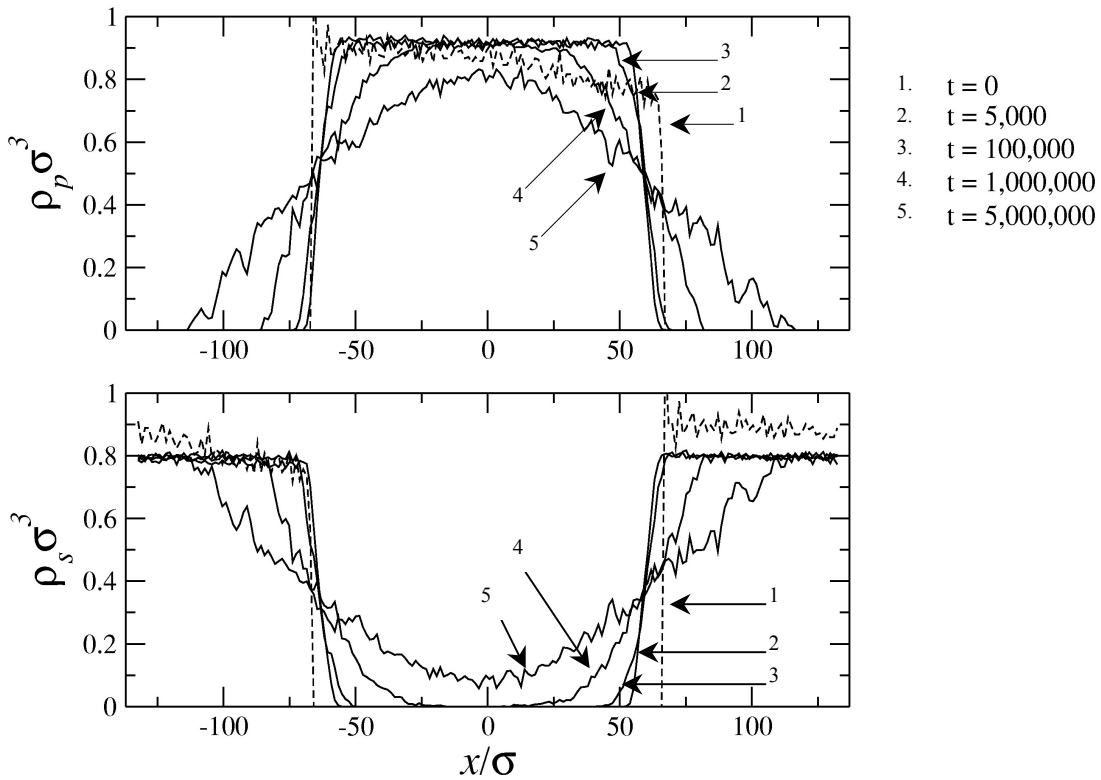


Figure 2 Plot of polymer (top) and solvent (bottom) density profiles for the case ($N = 100$, $N_{tot} = 40,000$). See Fig. 2.

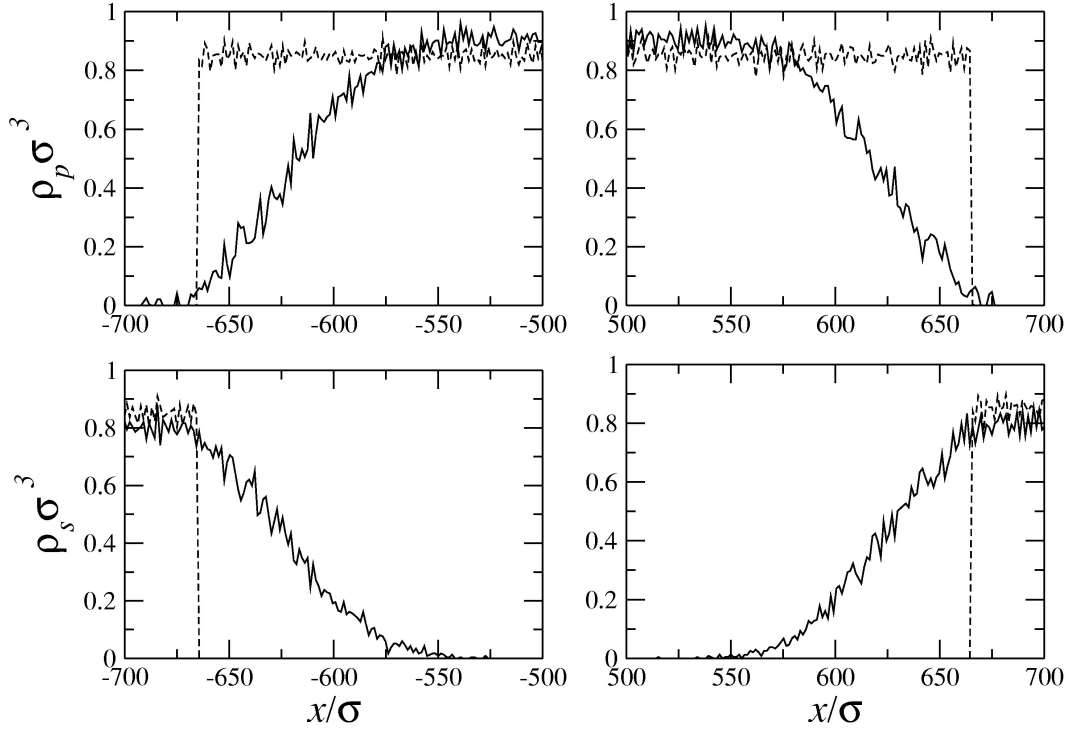


Figure 3 Plot of polymer (top) and solvent (bottom) density profiles for the case ($N = 10$, $N_{tot} = 400,000$). Only the left and right interfacial regions are plotted. The dashed lines show the density profile of the starting configuration. The solid lines are the density profiles after 11 million timesteps. One timestep corresponds to 0.005τ .

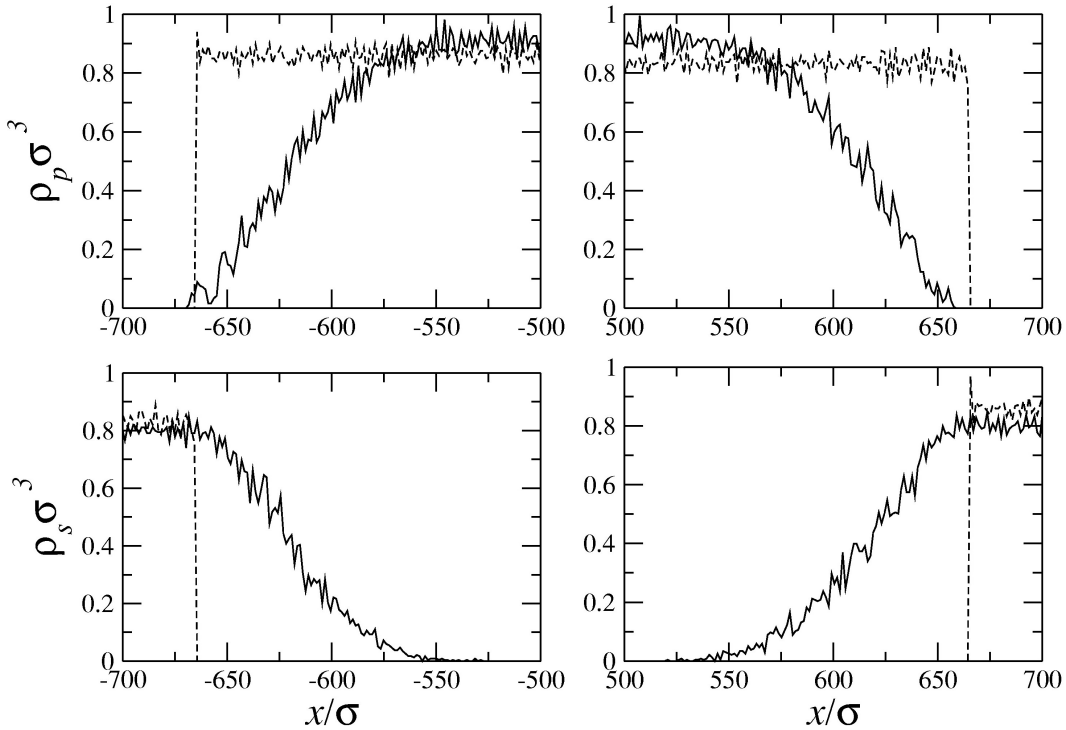


Figure 4 Plot of polymer (top) and solvent (bottom) density profiles for the case ($N = 100$, $N_{tot} = 400,000$). See Fig. 4.

Results

During each simulation, particle positions were written to a configuration data file. Fig. 1 shows a sequence of snapshots of the polymer and solvent positions for the case ($N = 100$, $N_{tot} = 4,000$). Because of the small system size, the polymer and solvent phases quickly penetrate the full thickness of the other phase. To study behavior at longer times, we then performed the same simulations with samples that were 10 times and 100 times thicker. For the larger systems, configurations were stored every 10,000 timesteps for the first million timesteps and every 100,000 timesteps thereafter. These data files were then used to construct solvent and polymer density profiles as a function of time. An example of such a time trace is shown in Fig. 2 for the case ($N = 10$, $N_{tot} = 40,000$). Several interesting features can be observed. At short and intermediate times both the solvent and polymer profiles exhibit error function tails which are characteristic of Fickian diffusion. At the longest times both the solvent and polymer components have penetrated the full film thickness of the other component. Comparison of the initial profile with the profile at timestep 1000 shows that the system underwent a rapid displacement in the early stage of the simulation. This was because the solvent and polymer phases were not initially at mechanical equilibrium. Due to intrachain bonding, the pressure in the polymer phase was somewhat lower than in the solvent phase at the same density. As a result, the polymer film compressed somewhat and the solvent phase expanded.

Fig. 3 shows the corresponding profiles for the case ($N = 100$, $N_{tot} = 40,000$). The solvent profiles once again exhibit Fickian tails. The penetration depth is somewhat less than for the shorter polymer chains. The polymer profiles appear to show more of a sharp front than a tail, suggesting the formation of a boundary between the solvent and swollen polymer regions.

Fig. 4 and 5 show the initial and long time density profiles for the 400,000 atom systems. In this case, the interfacial region only occupies a small fraction of the total box length, and so only the interfacial regions have been plotted. For the case $N = 10$, both the solvent and polymer components exhibit profiles characteristic of Fickian diffusion. In the case $N = 100$, the polymeric nature of the polymer component has become apparent. There is no inflection point in the polymer density profile.

We analyzed the interdiffusion by measuring the depth of penetration as a function of time. We define the location of the polymer and solvent fronts as the point where the concentration of each component drops below $\rho_{pen} \equiv 0.2\sigma^{-3}$. An example of the resultant front trajectory is shown in Fig. 6. The slowly decaying oscillations in the front positions are due to traveling pressure waves caused by the initial pressure imbalance between the solvent and polymer layers. These pressure waves did not show up in the 40,000 atom simulations, presumably because the characteristic wavelength was longer than the periodic box length. The amplitude of the oscillations decayed by about an order of magnitude from the beginning to the end of the simulation. The diffusion behavior was consistent throughout each simulation (see below), and so we conclude that the oscillations had no effect on diffusion behavior.

We defined the following average penetration depth, using both components and both the left and right interfaces

$$x_{pen} = \frac{1}{2} \left[\frac{1}{2} |x_{p,l} - x_{s,l}| + \frac{1}{2} |x_{p,r} - x_{s,r}| \right] \quad (3)$$

where $x_{p,l}$, $x_{p,r}$, $x_{s,l}$, and $x_{s,r}$ are the locations of the polymer and solvent fronts on the right and left interfaces, respectively. For comparison, we model the evolution of the polymer and solvent concentration profiles as ideal Fickian diffusion into a semi-infinite slab, for which the analytic solution is¹⁰

$$\rho(x,t) = \frac{\rho_0}{2} \operatorname{erfc}\left(\frac{x}{2\sqrt{Dt}}\right) \quad (4)$$

where t is time, x is distance from the interface, ρ is the concentration of either component, ρ_0 is the concentration in the pure phase, and D is the diffusivity. Inverting this equation we can write x_{pen} as a linear function of $t^{1/2}$.

$$x_{pen} = 2 \operatorname{erfc}^{-1}\left(\frac{2\rho_{pen}}{\rho_0}\right) \sqrt{Dt} \quad (5)$$

In Fig. 7 we plot x_{pen} versus $t^{1/2}$ for the 100 segment polymers with $N_{tot} = 40,000$ and $N_{tot} = 400,000$. The linear relationship with zero intercept provides clear evidence that in both cases the interdiffusion of the polymer and solvent is well represented by the ideal Fickian diffusion model. In particular, there is no evidence of an induction period or formation of an interphase between the solvent and the polymer phases. The most surprising result is the significantly slower rate of penetration for the larger system. To quantify this, we assumed $\rho_0 = 0.85\sigma^{-3}$ in Eq. 5, and calculated diffusivities for the 40,000 particle and 400,000 particle simulations. The polymer and solvent films in the 4,000 atom simulations were too thin to extract a diffusivity. The results are given in Table 1. The 400,000 atom simulations exhibit substantially lower diffusivities than the 40,000 atom simulations. In addition there was a small decrease in diffusivity in going from $N = 10$ to $N = 100$.

The strong effect of system size on diffusivity can not be attributed to thickness-induced differences in the polymer films, since it occurred for both entangled and unentangled polymers. Instead, we believe the cause is density changes induced by adding an interface to the system at constant volume. This can be seen from the data in Fig. 8, which shows the time variation of the polymer and solvent densities in the core region of each phase, for $N_{tot} = 40,000$. In the first 1000 timesteps, there was a rapid compression of the polymer and expansion of the solvent, as described above. After this, for a period of about 500,000 timesteps, the solvent density rises and the polymer density falls. The densities then reach a plateau until the core region is penetrated by the other species, at which point the densities start to decrease from the plateau value. This behavior was not observed in the 400,000 particle simulations (not shown). Apart from the slowly decaying oscillations due to pressure waves, the core densities remained constant throughout the simulations. The time average values from the 400,000 atom simulations are displayed as horizontal lines in Fig. 8.

This system-size dependence can be explained by the fact that the solvent near the interface is somewhat denser than the bulk solvent density far from the interface. In the case of the 40,000 particle simulations, the interfacial region occupies a substantial portion of the total simulation volume, and so results in a corresponding expansion of the polymer phase, since the total volume is conserved. In the case of the 400,000 particle simulations, the effect of the interface on the core polymer density is much weaker, because the volume occupied by the interfacial region is only a small fraction of the total system volume.

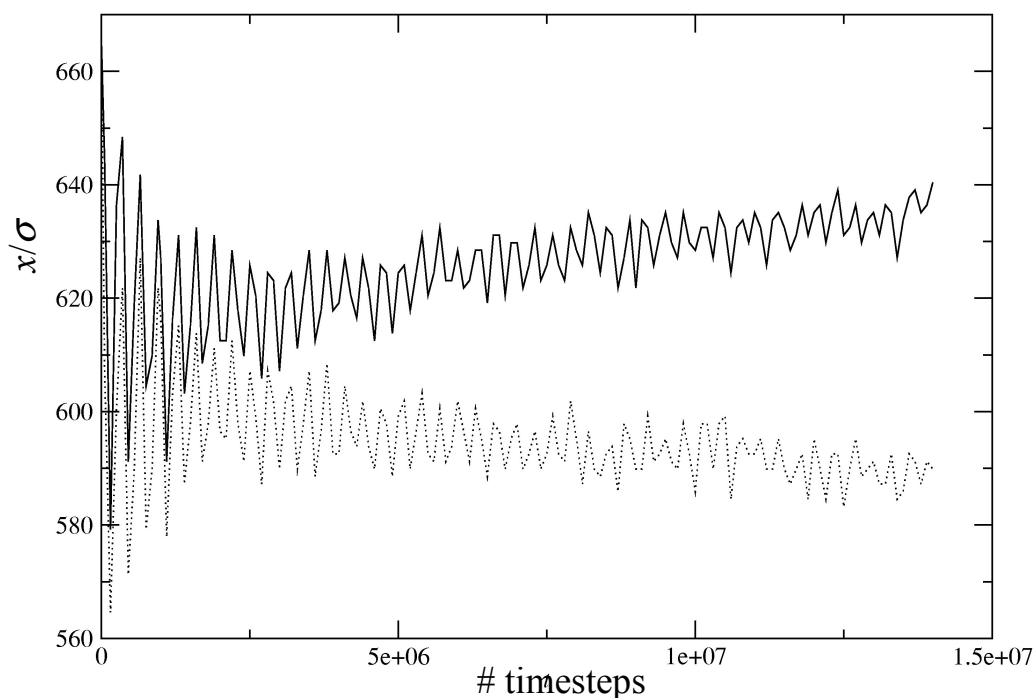


Figure 5 Plot of locations of the polymer (full line) and solvent (dotted line) fronts at the right interface versus time for the case ($N = 100$, $N_{tot} = 400,000$)

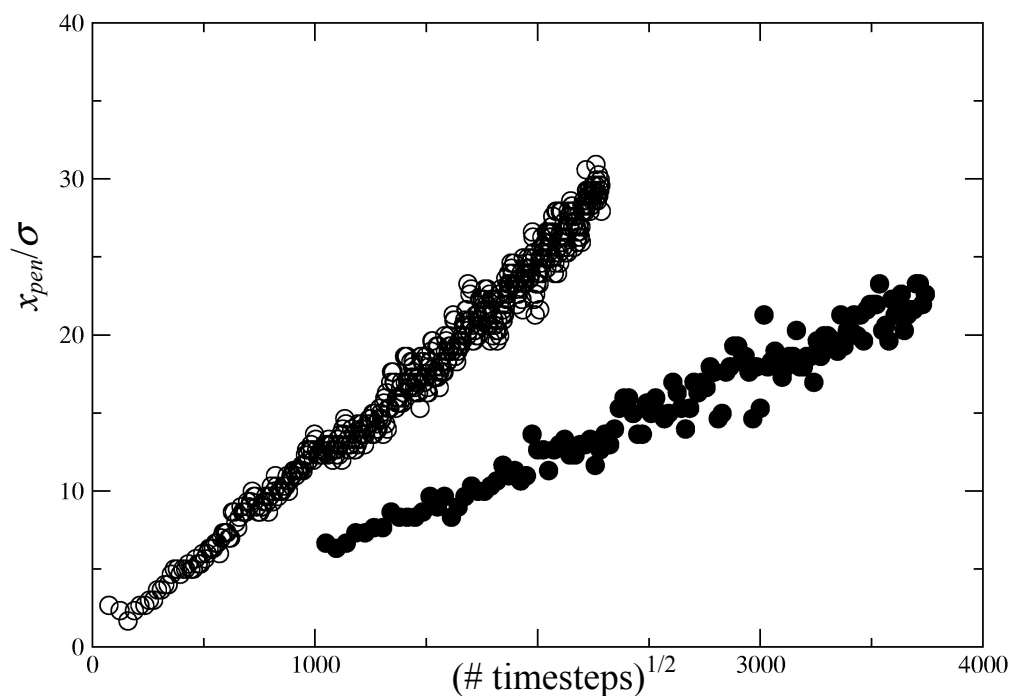


Figure 6 Plot of average penetration depth versus square root time for the cases ($N = 100$, $N_{tot} = 40,000$) (open circles) and ($N = 100$, $N_{tot} = 400,000$) (filled circles)

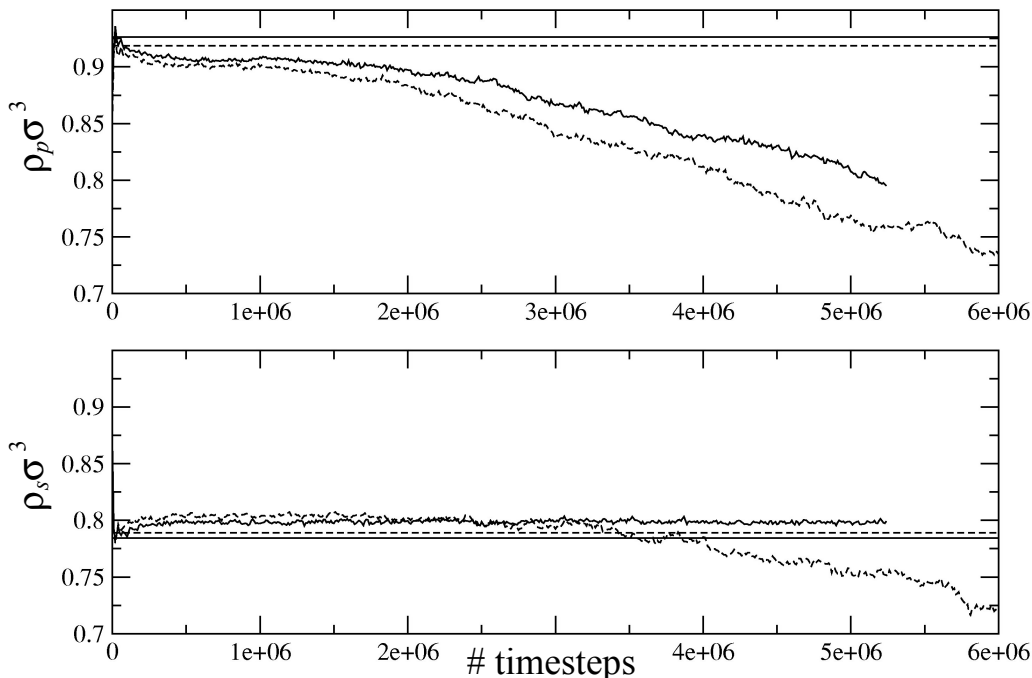


Figure 7 Plot of polymer density (top) and solvent density (bottom) versus time in the core regions. Results are shown for the 40,000 particle simulation with $N = 10$ (dashed line) and $N = 100$ (solid line). The horizontal lines are the corresponding time averages from the 400,000 particle simulations. The polymer densities were averaged on the range $(-10\sigma, 10\sigma)$ for $N_{tot} = 40,000$ and $(-200\sigma, 200\sigma)$ for $N_{tot} = 400,000$. The solvent densities were averaged on the range $(123\sigma, -123\sigma)$ for $N_{tot} = 40,000$ and $(1100\sigma, -1100\sigma)$ for $N_{tot} = 400,000$. One timestep corresponds to 0.005τ . The initial density was $0.85\sigma^{-3}$ in all cases.

The plateau values of the polymer core density $\rho_{p,eff}$ are given in Table 1. It is clear that the core polymer densities in the 40,000 particle simulations were significantly lower than those of the 400,000 particle simulations. We believe that this is the cause of the smaller diffusivities in the larger system. Interestingly, there is also a small effect of chain length on the core density. The roughly 10% increase in the number of bonds between the 10 segment and 100 segment chains caused a contraction of the polymer film and expansion of the solvent. The increased core density of the longer chains may account for most of the small decrease in diffusivity relative to the shorter chains.

Conclusions

The goal of this work was to look for non-Fickian behavior in the early stage of polymer dissolution. On the contrary, the analysis of the data in the previous section shows conclusively that the initial stage of dissolution conforms well to the Fickian model. Moreover, going from a non-entangled to an entangled melt did not cause any reduction in diffusivity, beyond that expected by the accompanying increase in bulk polymer density. The large reduction in diffusivity in going to a thicker film was also probably due to the significant increase in bulk polymer density. Hence, for the current polymer/solvent model, non-Fickian effects will occur, if at all, at much longer time and length scales, putting them beyond the reach of current molecular dynamics simulation capabilities. This does not rule out the possibility of simulating

interesting dissolution behavior using a different model, e.g. lowering the temperature to render the polymer glassy. One unexpected aspect of this work was the importance of controlling the polymer and solvent densities during the course of the simulation. This could be done by using volume fluctuations to maintain constant pressure. The use of grand canonical molecular dynamics would be even more effective, as it has the added benefit of eliminating the need for a large solvent reservoir.¹¹

References

1. J. M. Hruby "LIGA Technologies and Applications," *MRS Bulletin*, April 2001.
2. S. K. Griffiths, J. M. Hruby, and A. Ting, "The Influence of Feature Sidewall Tolerance on Minimum Absorber Thickness for LIGA X-Ray Masks," *Journal of Micromechanical Microengineering*, **9** 353 (1999).
3. G. Rossi, P. A. Pincus, and P.-G. de Gennes, "A Phenomenological Description of Case-II Diffusion in Polymer Materials," *Europhys. Lett.*, **32** 391 (1995).
4. B. Narasimhan and N. A. Peppas, "The Physics of Polymer Dissolution: Modeling Approaches and Experimental Behavior," *Adv. Polym. Sci.*, **128** 157 (1997).
5. H. F. Herman and S. F. Edwards, "A Reptation Model for Polymer Dissolution," *Macromolecules*, **23** 3662 (1990).
6. K. Kremer and G. S. Grest, "Dynamics of Entangled Linear Polymer Melts: a Molecular Dynamics Simulation," *J. Chem. Phys.*, **92** 5057 (1990).
7. B. Dunweg and K. Kremer, "Molecular Dynamics Simulation of a Polymer Chain in Solution," *J. Chem. Phys.*, **99** 6983 (1993).
8. S. J. Plimpton, R. Pollock, M. Stevens, "Particle-Mesh Ewald and rRESPA for Parallel Molecular Dynamics Simulations", in *Proc of the Eighth SIAM Conference on Parallel Processing for Scientific Computing*, Minneapolis, MN, March 1997.
9. R. Brightwell, L. A. Fisk, D. S. Greenberg, T. Hudson, M. Levenhagen, A. B. Maccabe, and R. Riesen, "Massively Parallel Computing using Commodity Components," *Parallel Comput.*, **26** 243 (2000).
10. J. Crank, *The Mathematics of Diffusion*, 2nd ed., Clarendon Press, 1979.
11. M. G. Martin, A. P. Thompson and T. M. Nenoff, "Effect of Pressure, Membrane Thickness, and Placement of Control Volumes on the Flux of Methane through Thin Silicalite Membranes: A Dual Control Volume Grand Canonical Molecular Dynamics Study," *J. Chem. Phys.*, **114** 7174 (2001)

The following people have received this information as a memorandum 11/08/2002
Distribution List

- 1 MS 0316 Steven Plimpton, 09209
- 1 MS 0316 Sudip Dosanjh, 09233
- 1 MS 0316 Rodney Schmidt 09233
- 5 MS 0316 Aidan Thompson, 09235
- 1 MS 0316 John Aidun, 09235
- 1 MS 0316 Mark Stevens, 09235
- 1 MS 0318 Paul Yarrington, 09230
- 1 MS 1349 John Curro, 01834
- 1 MS 1415 Gary Grest, 01114
- 1 MS 9003 Charles Hartwig, 08907
- 1 MS 9042 Stewart Griffiths, 08728
- 1 MS 9401 Jill Hruby, 08702
- 1 MS 9401 Craig Henderson, 08729
- 1 MS 9403 William Even, Jr., 08722
- 1 MS 9018 Central Technical Files, 8945-1
- 2 MS 0899 Technical Library, 9616
- 1 MS 0612 Review and Approval Desk, 9612 for DOE/OSTI